The significance and impact of incorporating a 3D point source in Green's theorem deghosting

Xinglu Lin and Arthur B. Weglein, M-OSRP/Physics Dept./University of Houston*

SUMMARY

The Green's theorem deghosting method (Weglein et al., 2002; Zhang and Weglein, 2005) provides useful/effective deghosted results if the nature of the 3D source is incorporated into the algorithm. For a 3D point source and a 1D subsurface, the method requires a single shot record with a complete 2D areal coverage of receivers. In this paper, a modified 3D source Green's theorem deghosting method is proposed for a 1D subsurface by employing polar coordinates and then reducing the areal integrals to an integral along the radial direction. Thereby, the modified method only requires one line of receivers with off-end shooting. The numeric results demonstrate that the modified method can achieve the objectives of ghost removal and restoring the source spectrum using one-streamer data on horizontal and non-horizontal cables.

INTRODUCTION

Methods for deghosting have a long history in seismic exploration with continued high interest in the topic and in achieving greater deghosting capability. The goal of this task is to remove the events that start their history as a wave moving up from the source (source-side ghost) or moving down to the receiver when it is recorded (receiver-side ghost), or both (source-receiver-side ghost). The process of deghosting is crucial for two reasons. Firstly, ghost events lead to the notches in the data spectrum, which can generate a serious issue at low-frequency part (close to zero frequency) (e.g., Zhang, 2007). The low-frequency information plays an important role in improving seismic resolution and subsequent inversion. Secondly, the success of deghosting is a pre-requisite for many processing algorithms including ISS free-surface multiple elimination and ISS internal multiple attenuation/elimination (Carvalho, 1992; Araújo, 1994; Weglein et al., 1997; Zou and Weglein, 2014).

A wave theoretic method - Green's theorem deghosting method - has been pioneered and developed by Weglein et al. (2002); Zhang and Weglein (2005); Zhang (2007); Mayhan and Weglein (2013); Weglein et al. (2013a) for off-shore plays and Tang (2014); Wu and Weglein (2014) for on-shore plays. This deghosting method works in the space-frequency domain for multidimensional data. Mayhan (2013) provides positive deghosted results for both 2D line source and 3D point source marine data by applying a complete Green's theorem deghosting method. However, a complete method has certain requirements for certain source dimension. Consider a 3D source deghosting as an example due to the reality of source dimension. Even for a 1D earth, 3D Green's theorem deghosting method needs an areal coverage of 3D source data, which challenges acquisition and computation. Mayhan (2013) proposed to utilize the local property of Green's function to reduce the need of input data, where an areal coverage is still required. The other method, which can be compared with Green's theorem derived deghosting method, is a conventional $P-V_z$ sum method of deghosting in the wavenumber-frequency domain (Amundsen, 1993; Robertsson and Kragh, 2002). Given a 3D source acquisition on a horizontal streamer coming from a 1D earth, Amundsen (1993) applied a forward and an inverse Hankel transform to deghost in the wavenumber-frequency domain. Although this method can process a line acquisition with off-end shooting at one time, the application of this $P-V_z$ sum assumes a dense sampling on a horizontal cable to support an effective Hankel transform. Compared to the Green's theorem derived deghosting method, this method has the limitations of measurement surface, which can generate issues for dipping-cable, ocean-bottom and on-shore data deghosting (Weglein et al., 2013b).

Due to the advantage of Green's theorem deghosting, we start from a complete 3D Green's theorem derived deghosting algorithm, which stays in the space-frequency domain, and then reduce the earth dimension from 3D to 1D for receiver-side-deghosting. The reduced/modified algorithm can deghost one line of receivers with off-end 3D source shooting at one time without any assumption of cable shape. Numerical tests are performed on synthetic 3D source/1D subsurface data that are recorded on horizontal and non-horizontal cables.

GREEN'S THEOREM DERIVED DEGHOSTING

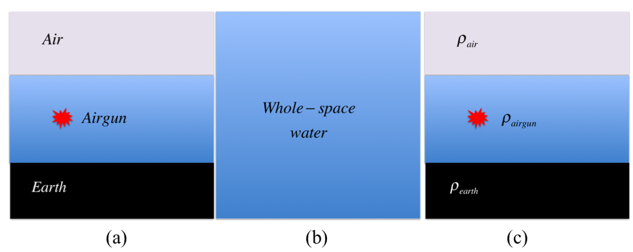

Figure 1: (a) Actual medium; (b) Reference medium; (c) Three sources (air, airguns, and earth) overlaid on reference medium.

To achieve the objective of deghosting in marine case (figure 1 (a)), a whole space of water is selected as a reference medium (figure 1 (b)), in which the Green's function is analytically known (chapter 7, Morse and Feshbach (1953)). The differences between actual and reference properties are characterized by ρ terms in figure 1 (c). For this choice of reference medium, active source (e.g., airguns) and passive sources (e.g., air, earth) contribute to the total wavefield at space point $\mathbf{r}$ as,

$$P(\mathbf{r},\omega) = \int_\infty d\mathbf{r}'\rho(\mathbf{r}',\omega)G_0^+(\mathbf{r},\mathbf{r}',\omega)$$
$$= \int d\mathbf{r}'\rho_{air}G_0^+ + \int d\mathbf{r}'\rho_{airguns}G_0^+ + \int d\mathbf{r}'\rho_{earth}G_0^+, \quad (1)$$

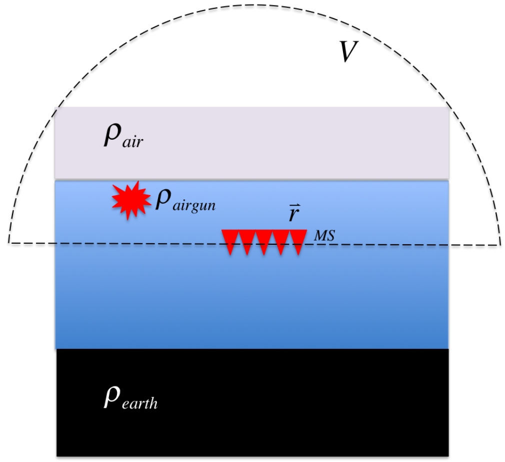

Figure 2: Configuration for receiver-side deghosting.

where G_0^+ is a causal Green's function for the reference medium.

Choosing an enclosed volume V that is bound by surface S and a causal Green's function, Weglein and Secrest (1990) has shown that the Green's second identity derived integral

$$\oint dS\hat{n}\cdot\{P(\mathbf{r}',\omega)\nabla G_0^+(\mathbf{r},\mathbf{r}',\omega)-G_0^+(\mathbf{r},\mathbf{r}',\omega)\nabla P(\mathbf{r}',\omega)\} \quad (2)$$

identifies the contribution to the wavefield P recorded inside volume V due to the sources located outside the volume V, where the $\hat{n}$ is an unit vector that is normed to S and points to the outside of boundary. $\mathbf{r}$ is the prediction point and $\mathbf{r}'$ is the measurement point. In deghosting task, we choose a hemisphere above the measurement surface as shown in figure 2. Since the chosen volume V encloses air and airguns, the only outside contribution to the inside point comes from the earth beneath the water-bottom. When this hemisphere is large enough, the integral over the shell part vanishes by applying the sommerfeld radiation condition and the integral over the measurement surface lives. We can predict the receiver-side deghosted data P^{rd} at location $\mathbf{r}$ by applying,

$$P^{rd}(\mathbf{r},\omega)=\int\rho_{earth}G_0^+=\int_{MS}dS\hat{n}\cdot\{P\nabla G_0^+-G_0^+\nabla P\}, \quad (3)$$

where $\mathbf{r}$ is above the measurement cable and beneath the source point (in the chosen volume).

MODIFIED 3D SOURCE GREEN'S THEOREM DEGHOSTING FOR A 1D SUBSURFACE

When a horizontal measurement surface is assumed, a complete 3D Green's theorem deghosting method has been proposed and pioneered by Weglein et al. (2002) and Zhang (2007) as,

$$P^{rd}(x,y,z,\omega)=\int\int\{P(x',y',z',\omega)\frac{\partial G_0^{3D}(x,y,z,x',y',z',\omega)}{\partial z'} -G_0^{3D}(x,y,z,x',y',z',\omega)\frac{\partial P(x',y',z',\omega)}{\partial z'}\}dx'dy', \quad (4)$$

where $G_0^{3D}(x,y,z,x',y',z',\omega)=-\frac{e^{ikR}}{4\pi R}$, $k=\frac{\omega}{c_0}$, $R=\sqrt{(x-x')^2+(y-y')^2+(z-z')^2}$. This comprehensive 3D deghosting method can process any 3D source data with an areal coverage of receivers as input.

Based on this original 3D Green's theorem deghosting algorithm, we derive the modified 3D source/1D subsurface Green's theorem deghosting method in cylindrical coordinates. The description of location can be changed from (x,y,z) to (r,θ,z) or $(\mathbf{r},z)$. Setting the differential vectors as $\mathbf{r_h}=\mathbf{r}-\mathbf{r_s}$ and $\mathbf{r'_h}=\mathbf{r}'-\mathbf{r_s}$, where $\mathbf{r_h}=(r_h,\theta_h)$ and $\mathbf{r'_h}=(r'_h,\theta'_h)$, we can reduced the dependance of data to $P(r_h,z,\omega)$ for 1D subsurface. The equation (4) can be rearranged to,

$$\begin{aligned} &P_{1D}^{rd}(r_h,z,\omega) \quad (5)\\ &=\int_0^{2\pi}\int_0^{+\infty}\{P_{1D}(r'_h,z',\omega)\frac{\partial G_0^{3D}(r_h,\theta_h,z,r'_h,\theta'_h,z',\omega)}{\partial z'}\\ &-G_0^{3D}(r_h,\theta_h,z,r'_h,\theta'_h,z',\omega)\frac{\partial P_{1D}(r'_h,z',\omega)}{\partial z'}\}r'_h dr'_h d\theta', \end{aligned}$$

where

$$G_0^{3D}(r_h,\theta_h,z,r'_h,\theta'_h,z',\omega)=-\frac{e^{ik\sqrt{r_h^2+r_h'^2-2r_hr'_hcos(\theta_h-\theta'_h)+(z-z')^2}}}{4\pi\sqrt{r_h^2+r_h'^2-2r_hr'_hcos(\theta_h-\theta'_h)+(z-z')^2}}.$$

P_{1D} and P'_{1D} come out of the integral over azimuth angle θ'. The modified 3D source/1D subsurface Green's theorem deghosting algorithm becomes,

$$P_{1D}^{rd}(r_h,z,\omega)=\int_0^{+\infty}\{P_{1D}(r'_h,z',\omega)IG'_0(r_h,z,r'_h,z',\omega)- IG_0(r_h,z,r'_h,z',\omega)\frac{\partial P_{1D}(r'_h,z',\omega)}{\partial z'}\}r'_h dr'_h, \quad (6)$$

where IG_0 and IG'_0 are the azimuthal integrals of whole-space water Green's function and its first derivative respect to z'. IG'_0 and IG_0 can be expressed as,

$$\begin{aligned} &IG'_0(r_h,r'_h,|z-z'|,\omega) \quad (7)\\ &=\frac{z-z'}{4\pi}\int_0^{2\pi}(ik\sqrt{a-bcos\theta}-1)\frac{e^{ik\sqrt{a-bcos\theta}}}{(\sqrt{a-bcos\theta})^3}d\theta \end{aligned}$$

and

$$IG_0(r_h,r'_h,|z-z'|,\omega)=\frac{-1}{4\pi}\int_0^{2\pi}\frac{e^{ik\sqrt{a-bcos\theta}}}{\sqrt{a-bcos\theta}}d\theta, \quad (8)$$

where $a=r_h'^2+r_h^2+(z-z')^2$ and $b=2r'_hr_h$. Equation (6) states that when the earth varies in 1D the algorithm sum over the weights (values of Green's function or its derivative) from different azimuthal angles first for a fixed radial length. And then it integrates over all different radial length along offset, which involves the data at different offsets.

Since the Green's theorem deghosting stays in the space-domain, the input data do not have to be recorded on a horizontal surface or cable. If a curved cable is chosen, the receiver-geometry leads to a correction on the equation (6) as,

$$\begin{aligned} P_{1D}^{rd}(r_h,z,\omega)=\int_0^{+\infty}&\{P_{1D}(r'_h,z',\omega)IG'_0(r_h,z,r'_h,z',\omega)\\ &-IG_0(r_h,z,r'_h,z',\omega)\frac{\partial P_{1D}(r'_h,z',\omega)}{\partial n}\}\\ &\times\sqrt{1+\left(\frac{df(r'_h)}{dr'_h}\right)^2}r'_h dr'_h, \quad (9) \end{aligned}$$

where IG_0 and IG_0' are the azimuthal integrals of whole-space water Green's function and its first derivative respect to $\hat{n}$, $z' = f(r_h')$ is a acquisition geometry function. IG_0' and IG_0 can be expressed as $IG_0' = \frac{-1}{4\pi}\int_0^{2\pi}\frac{\partial G_0}{\partial n}d\theta$ and $IG_0 = \frac{-1}{4\pi}\int_0^{2\pi}G_0 d\theta$. The normal direction $\hat{n}$ points to the outside of the volume. To predict the up-going components at any point above the curved cable, we need the P, $\partial P/\partial n$ along the curved cable and the acquisition geometry $f(r_h')$ as input.

NUMERICAL RESULTS

Synthetic 3D source data are generated by using reflectivity method from a 1D layered medium. In order to avoid the error from the derivative of P, we analytically calculate the $\partial P/\partial n$ as one of the inputs. In practice, the $\partial P/\partial z'$ can be obtained by dual-sensor streamers (e.g., PGS) or over/under streamers (e.g., Schlumberger).

3D source deghosting on a horizontal cable

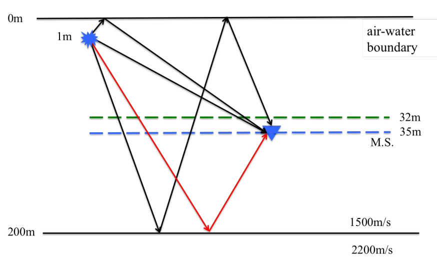

Figure 3: Acoustic model used for numerical tests. Synthetic data contains direct wave, ghost of the direct wave, primary event and receiver-side ghost of the primary event. The dashed blue line represents the location of measurement streamer and the dashed green line represents the location of predicted/output streamer.

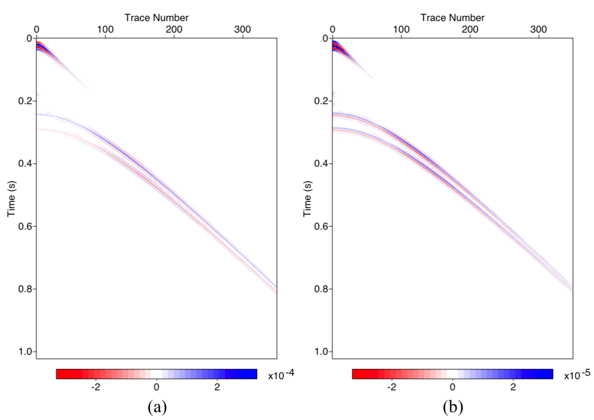

Figure 4: (a) Synthetic data P; (b) $\partial P/\partial z'$ at depth 35m.

The 3D source data, recorded on a horizontal streamer, is generated by model in figure 3. This dataset contains direct wave, ghost of the direct wave, primary and ghost of the primary. After deghosting, the only event left in result is expected to be the scattered wave from earth (primary event), which is represented by the red ray-path in figure 3. The original 3D source data and its derivative respect to $+z$ are presented in figure 4 (a) and (b) as inputs.

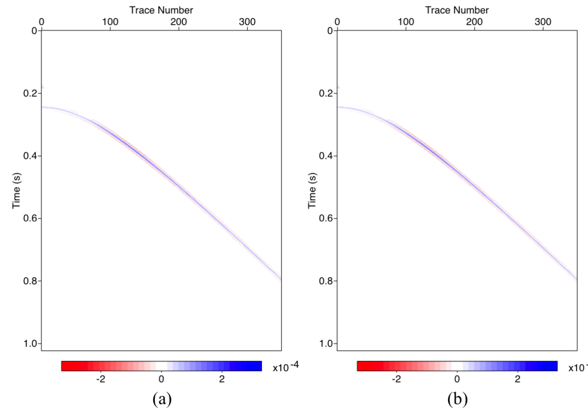

Figure 5: (a) Simulated primary event; (b) Deghosted result by using the modified 3D source Greens theorem at depth 32m.

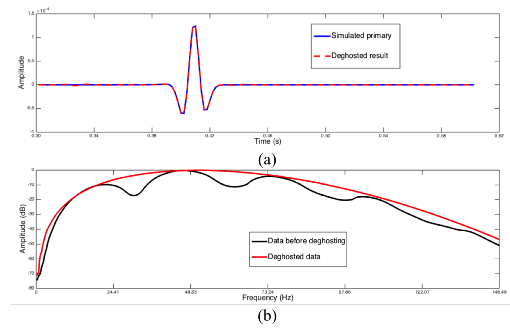

Figure 6: Results by using modified 3D source/1D subsurface Green's theorem deghosting method: (a) Wiggle comparison on trace 150 of simulated primary event and deghosted data; (b) Spectrum comparison between input data (with ghost) and deghosted data.

By applying the equation (6), the shot gather in figure 4 can be deghosted at the depth (32m) shallower than original cable (35m). The primary-only data are simulated so as to compare with the deghosted result in figure 5 (a). The deghosted result is shown in figure 5 (b). Comparing these two shot gather plots, we can hardly detect any difference between them, which means that the 3D source/1D subsurface Green's theorem deghosting can successfully remove the direct wave and the ghosts. The wiggle plot in figure 6 (a) compares the deghosted result (dashed red line) with the simulated primary event (blue line) on trace 150. The overlapped two lines indicate that the deghosting method can also restore the primary event. Figure 6 (b) provides the average spectrum of input data (with direct wave and ghosts, black line) and deghosted data (red line). The notches in original data can be boosted and the low-frequency information can be recovered after deghosting.

3D source deghosting on a curved cable

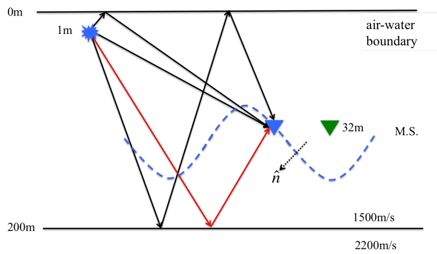

Figure 7: Acoustic model used for numerical tests. Synthetic data contains direct wave, ghost of the direct wave, primary event and receiver-side ghost of the primary event. The dashed blue line represents the location of measurement streamer and the green triangle represents the location of predicted/output point.

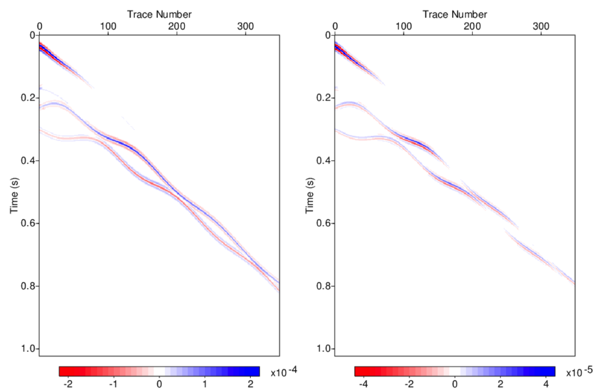

(a) (b)

Figure 8: (a) Synthetic data P; (b) $\partial P/\partial n$ on a curved cable.

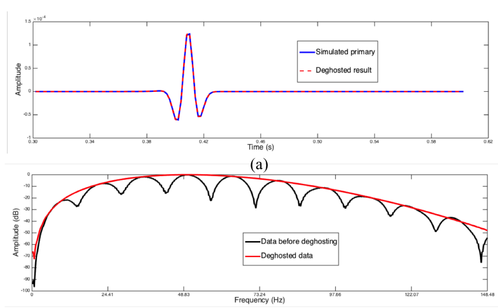

(a)

(b)

Figure 9: Results by using modified 3D source/1D subsurface Green's theorem deghosting method: (a) Wiggle comparison on trace 150 between simulated primary event and deghosted data; (b) Spectrum comparison between input data (with ghost) and deghosted data.

Since the Green's theorem deghosting stays in coordinate space, the method can deal with the shot gather from a non-flat cable. In order to show its advantages, the second numerical test is performed on a dataset that is recorded on a curved cable. Figure 7 provides the acoustic model and receiver geometry we used to generate the data, where the curved cable is represented by a blue dashed line. In this experiment, we output the deghosted data on one receiver located above the curved cable, which is represented by the green triangle in figure 7. The inputs 3D source P on curved cable and $\partial P/\partial n$ has been presented in figure 8 (a) and (b).

The deghosted data (red line, in figure 9 (a)) can be predicted at the output point by using equation (9). In the same plot, the simulated primary event is provided by a solid blue line. These two events overlap each other, which illustrates a promising deghosted result. Figure 9 (b) gives a spectrum comparison between the input data (black line, with direct wave and ghost) and deghosted result (red line). Similar to the previously shown deghosted results on horizontal cable, the problem of notches can be solved after applying the modified 3D source Green's theorem deghosting method, which benefits the resolution in data spectrum. In other words, this method can accommodate the input data on curved cable well to provide an effective deghosted result for 3D source data.

CONCLUSION

Starting with a complete 3D Green's theorem derived deghosting method, a modified 3D deghosting method for a 1D subsurface is proposed to deghost one pre-stack line acquisition with off-end shooting in the (r,ω) domain. The numerical results illustrate that the modified algorithm (for receiver-side deghosting) can effectively remove the down-going events (e.g., direct wave, ghosts) and restore the up-going events at receivers for a horizontal or non-horizontal cable. This paper contributes to Green's theorem deghosting capability by retaining the realism of a 3D source and reducing data requirement and computation cost for data coming from a 1D subsurface. In addition, the issue in this paper is relevant for both broadband objectives and satisfying the prerequisite of ISS free-surface and internal multiple algorithms.

ACKNOWLEDGMENTS

We are grateful to all the M-OSRP sponsors for their long-term support and encouragements.